A Study on the Real-Time Parameter Estimation of DURUMI-II for Control Surface Fault Using Flight Test Data (Longitudinal Motion)

Wook-Je Park, Eung-Tai Kim, Yong-Kyu Song, and Bong-Jin Ko

Abstract: For the purpose of fault detection of the primary control surface, real-time estimation of the longitudinal stability and control derivatives of the DURUMI-II using the flight data is considered in this paper. The DURUM-II, a research UAV developed by KARI, is designed to have split control surfaces for the redundancy and to guarantee safety during the fault mode flight test. For fault mode analysis, the right elevator was deliberately fixed to the specified deflection condition. This study also mentions how to implement the multi-step control input efficiently, and how to switch between the normal mode and the fault mode during the flight test. As a real-time parameter estimation technique, Fourier transform regression method was used and the estimated data was compared with the results of the analytical method and the other available method. The aerodynamic derivatives estimated from the normal mode flight data and the fault mode data are compared and the possibility to detect the elevator fault by monitoring the control derivative estimated in real time by the computer onboard was discussed.

Keywords: Fault detection, flight test, longitudinal stability, real-time parameter estimation, uninhabited aerial vehicle (UAV).

1. INTRODUCTION

Typically, the maximum likelihood estimation [1] (MLE) is the most widely used algorithm for parameter estimation from flight test data [2-5]. It has been successfully used for both linear and nonlinear models. The parameters are estimated by maximizing the probability of correspondence between estimation and measurement data. The iterative algorithm of the maximum likelihood estimation is slower than algorithm of the extended Kalman filter (EKF) or the Fourier transform regression (FTR).

The basic approach of the extended Kalman filter [6-9] is the state estimation, which is the same in direct parameter estimation. The parameters are also considered as states in a filtering problem. It is no increment in difficulty associated with the parameter estimation of nonlinear systems, compared to that of linear systems. The extended Kalman filter is a one-pass algorithm, which usually means that it is faster than the algorithm of MLE and that it is applicable to the unstable and on-line systems. The extended Kalman filter requires the specification of initial values and error covariance for the estimate and the knowledge of measurement and process noise statistics.

In this paper, the Fourier transform regression [10-15] is proposed for the parameter estimation algorithm. It consists of suitably excited input and actually measured system responses; therefore, it is possible to be repeatedly implemented in UAV tests aboard in real time.

The algorithm of the EKF consists of arithmetical computations and twice matrices inversion, while the FTR algorithm involves arithmetical computations and three times matrices inversion. The FTR is simpler than the EKF equations. The FTR algorithm is slower than the EKF algorithm, because the arithmetical computational matrices inversions of FTR required computations of complex numbers. Both the FTR and EKF are applicable to on-line parameter estimation; however the EKF has the problem for sensitivity on initial values.

The FTR algorithm is preferably applied because of

Manuscript received March 23, 2006; revised October 11, 2006 and February 6, 2007; accepted April 6, 2007. Recommended by Editorial Board member Hyo-Choong Bang under the direction of Editor Jae Weon Choi. The authors would like to state their appreciation to the late Professor Myoung-shin Hwang and the late Professor Hee-Bong Eun, who initiated and contributed to the flight testing and data analysis of small aircraft of Korea.

Wook-Je Park is with the School of Mechatronics, Changwon National University, #9 Sarim-dong, Changwon 641-773, Korea (e-mail: parkwj@changwon.ac.kr).

Eung-Tai Kim is with Control and Avionics Group, Korea Aerospace Research Institute, 45 Eoeun-dong, Yuseong-gu, Daejon 305-333, Korea (e-mail: eungkim@kari.re.kr).

Yong-Kyu Song is with the School of Aerospace and Mechanical Engineering, Korea Aerospace University, Koyang-si 412-791, Korea (e-mail: yksong@hau.ac.kr).

Bong-Jin Ko is with the School of Mechatronics, Changwon National University, #9 Sarim-dong, Changwon 641-773, Korea (e-mail: bjko@changwon.ac.kr).

its rapid convergence and robustness to measurement and system noise while the EKF has the problem of sensitivity on initial values. Recently, the FTR is applied to the parameter estimation of an aircraft that experiences failure or is in damage state as well as in normal state. Typically, frequency range in rigid body dynamics such as the DURUMI-II can be selected for filtering out higher frequency noise and structural interference [11,12].

In the event of the control surface malfunction in flight, if the status of the damage is known, the fault tolerant control system is capable of adapting to the various faults in real time. Assuming the controllability and the trimmability of the aircraft at post-failure conditions, in the event of the control surface becoming jammed, the aircraft can keep on flying by the flight control computer, which has restructured and reconfigured controllers according to the grade of system failure. Without adding a sensor or additional cost, the advantage is an increase in reliability as the flight control system is reconfigured using on-line estimates of aircraft parameters from a real-time parameter estimation scheme. The aim of the research is to find the status of the failure by using the parameter estimation method in the case of a jammed control surface.

2. UNINHABITED AERIAL VEHICLE

To enhance the flight safety during failure mode test, the DURUMI-II, a research UAV developed by KARI, is designed to have redundancy in the control surface. The DURUMI-II is a 150% enlarged version of the DURUMI [16-19]. The specifications of the DURUMI-II are presented in Table 1. Figs. 2 - 4 show the changed configuration of the DURUMI-II. If any malfunction of the control surface should occur, this system will help the DURUMI-II to fly safely. The selection of flight mode between normal and failure state is remotely performed by handling the switch during the flights.

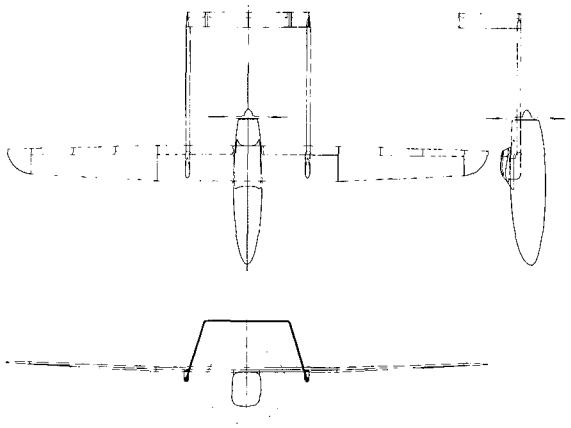

Fig. 1. DURUMI-II three views.

Table 1. DURUMI-II specifications.

Length	2.7m
Span	4.8m
Height	1.22m
Aspect Ratio	15
Powerplant	ZDZ80RV
Power	7.9hp
Maximum Take-off Weight	37kg
Gross Weight	22kg
Payload	12kg
Stall Speed	60km/h
Cruise Speed	125km/h
Maximum Speed	150km/h

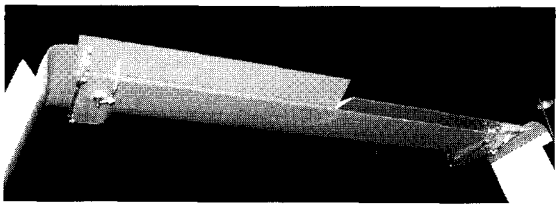

Fig. 2. Split in elevator.

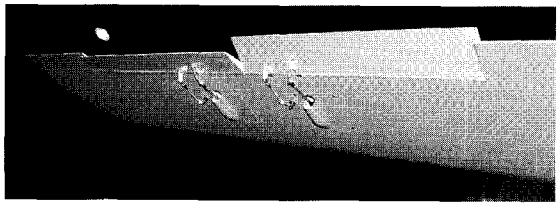

Fig. 3. Split in ailerons.

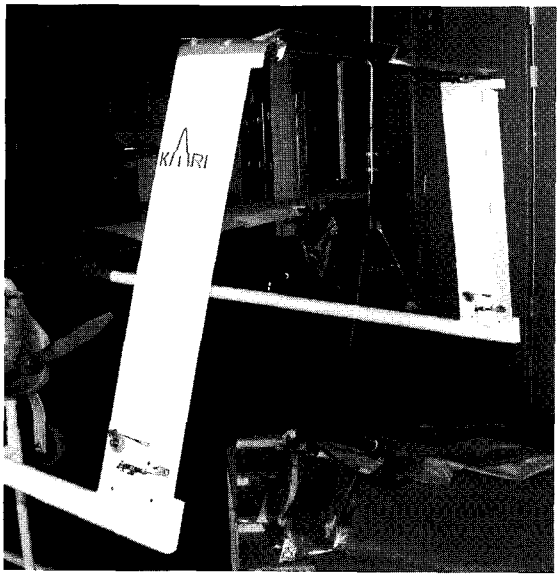

Fig. 4. Rudder added.

3. FLIGHT TEST

The DURUMI-II has been tested to obtain aerody-

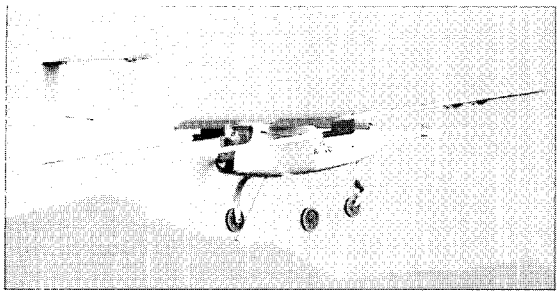

Fig. 5. DURUMI-II in take-off.

namic coefficients and control derivatives. Parameter estimation techniques depend on the control inputs exciting the dynamics of an airplane. A longitudinal mode can be excited by a simple pulse, doublet, multi-step input on the elevator. The commonly used flight test [2-5] techniques to obtain longitudinal stability data are relatively simple and straightforward. Lift coefficient and pitching moment coefficient can be estimated from a series of steady-state flight tests conducted under various center of gravity (C.G) conditions. The considerable efforts such as test pilot training and auto pilot programming are required to obtain statistically reliable flight data. To reduce the cost and time, the program mixing and switching method of the remote control transmitter is used to apply the exact control input. Fig. 5 shows the DURUMI-II in take-off phase.

3.1. Control input design and application

It is important to perform the flight test in order to find out the suitable control input, because the control input is exciting the dynamics of the aircraft. The input forms have the doublet, multi-step 2-1-1 and multi-step 3-2-1-1 input [2,5,11,20]. Fig. 6 indicates

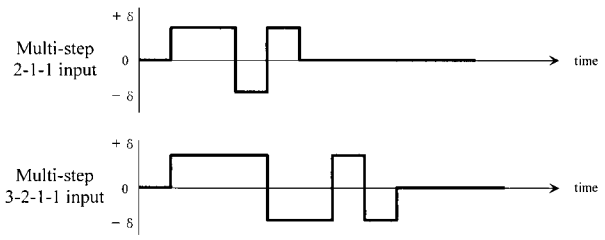

Fig. 6. Multi-step input.

the doublet, multi-step 2-1-1 and multi-step 3-2-1-1 input. However, many of these input forms have not been applied in the flight test for a number of reasons. As a result of first flight, the doublet input cannot produce the best response of the DURUMI-II. The time step is reduced from 1 sec to 0.7 sec. The multi-step 3-2-1-1 input is applied. Through the analysis of the flight test data of the DURUMI-II, the multi-step 3-2-1-1 input was proven to produce the best response of the DURUMI-II with a good amount of information concerning the aircraft dynamics for the estimation of stability and control derivatives.

The control input with designed amplitude excursion has been programmed in the R/C transmit device [21]. When the ground test pilot maintains a steady level flight, the flight test engineer applies the multi-step control input such as 3-2-1-1 by operating the switch. During the flight, it is very difficult for the ground test pilot to apply the control input that is close enough to the 3-2-1-1 or 2-1-1 input. Even repeated training for a long time would greatly help the pilot apply the control input with the required level of accuracy.

3.2. Flight test of normal mode and fault mode

The right-side elevator was fixed deliberately, and

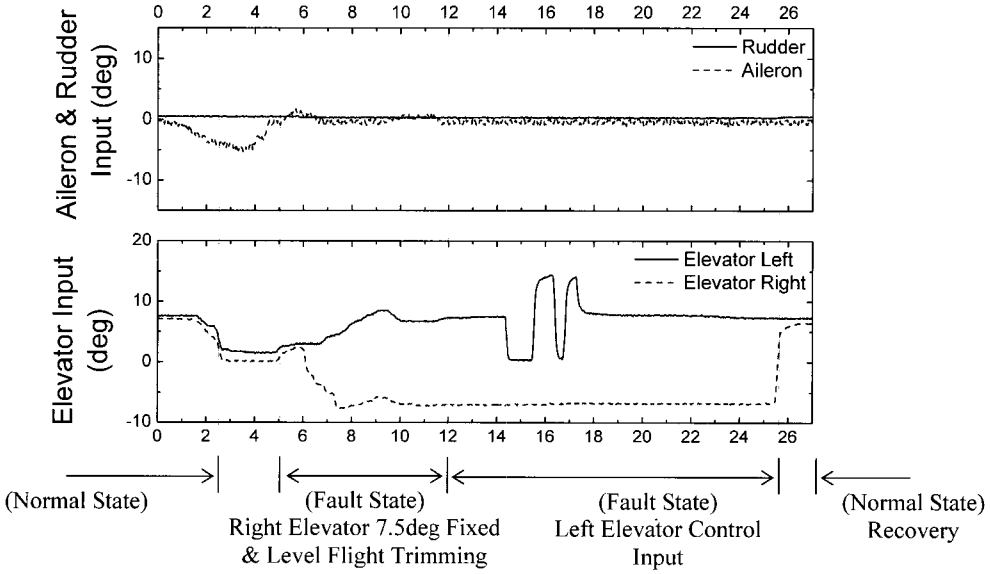

Fig. 7. Fault mode control input using switching method in flight.

Table 2. Flight test condition.

Flight condition	Fault condition	Control input
Normal mode	Elevator normal operation	3-2-1-1
Fault mode I	Right elevator fixed: 0deg	3-2-1-1
Fault mode II	Right elevator fixed: -7.5deg	3-2-1-1
Fault mode III	Right elevator fixed: -15deg	3-2-1-1
Fault mode IV	Right elevator fixed: +7.5deg	3-2-1-1
Fault mode V	Right elevator fixed: +15deg	3-2-1-1

aerodynamic coefficients and control derivatives were computed in real time by the computer onboard the DURUMI-II using the real-time parameter estimation method of Fourier transform regression. After realizing the scenario of right elevator fault by operating the knob and the switch, the ground test pilot maintains a steady level flight. The flight test engineer also applies the multi-step control input by operating the switch. Finally, after the flight maneuvering is completed, the flight test engineer restores the knob and the switch to a normal state position. Table 2 presents the five cases of flight test conditions including the fault state with a fixed right elevator. Fig. 7 shows the flight test procedure for the switch operation of normal mode and fault mode during a flight.

4. MODELING FORMULATION

Airplane dynamics can be described by the following linear modeling equations:

$$\dot{x}(t) = Ax(t) + Bu(t), \tag{1}$$

$$y(t) = Cx(t) + Du(t). \tag{2}$$

The dynamic system [10-12], whose parameters are to be estimated, has stability and control derivatives. The parameters to be estimated are assumed to be constant during the flight test maneuver.

The finite Fourier transform of a signal $x(t)$ is defined by

$$\tilde{x}(\omega) \equiv \int_0^T x(t)e^{-j\omega t}dt. \tag{3}$$

Applying the Fourier transform to (1) and (2) gives

$$j\omega\tilde{x}(\omega) = A\tilde{x}(\omega) + B\tilde{u}(\omega), \tag{4}$$

$$\tilde{y}(\omega) = C\tilde{x}(\omega) + D\tilde{u}(\omega). \tag{5}$$

When the states x, inputs u, and outputs y are measured, individual state or output equations from vector (4) or (5) can be used in an equation error formulation to estimate the stability and control derivatives contained in matrices A, B, C, and D.

For the k-th state equation of vector (4), the cost function is

$$J_k = \frac{1}{2}\sum_{n=1}^{m}\left|j\omega_n\tilde{x}_k(n) - A_k\tilde{x}(n) - B_k\tilde{u}(n)\right|^2. \tag{6}$$

Similar cost expressions can be written for (2)

$$Y = X\Theta + \varepsilon, \tag{7}$$

where

$$Y \equiv \begin{bmatrix} j\omega_1\tilde{x}_k(1) \\ j\omega_2\tilde{x}_k(2) \\ \vdots \\ j\omega_m\tilde{x}_k(m) \end{bmatrix}, \tag{8}$$

$$X \equiv \begin{bmatrix} \tilde{x}^T(1) & \tilde{u}^T(1) \\ \tilde{x}^T(2) & \tilde{u}^T(2) \\ \vdots & \vdots \\ \tilde{x}^T(m) & \tilde{u}^T(m) \end{bmatrix}, \tag{9}$$

and ε represents the equation error in the frequency domain. The least squares cost function is

$$J = \frac{1}{2}(Y - X\Theta)^*(Y - X\Theta), \tag{10}$$

$$\tilde{\Theta} = \left[\mathrm{Re}\left(X^*X\right)\right]^{-1}\mathrm{Re}\left(X^*Y\right). \tag{11}$$

The estimated parameter covariance matrix is

$$\begin{aligned}\mathrm{cov}\left(\tilde{\Theta}\right) &= E\left[\left(\tilde{\Theta} - \Theta\right)\left(\tilde{\Theta} - \Theta\right)^{-1}\right] \\ &= \sigma^2\left[\mathrm{Re}\left(X^*X\right)\right]^{-1},\end{aligned} \tag{12}$$

where the equation error variance can be estimated from the residuals,

$$\sigma^2 = \frac{1}{(m-p)}\left[\left(Y - X\hat{\Theta}\right)^*\left(Y - X\hat{\Theta}\right)\right], \tag{13}$$

where p is the number of elements in parameter vector $\tilde{\Theta}$.

For a given frequency ω, the discrete Fourier transform at sampling time i-th is defined by

$$X_i(\omega) = X_{i-1}(\omega) + x_i e^{-j\omega_i\Delta t}. \tag{14}$$

The quantity $e^{-j\omega_i\Delta t}$ is constant for a given frequency and constant sampling interval.

Rigid body dynamics of the DURUMI-II lie in the rather narrow frequency band of 0.01-1.5Hz. Consequently, it is possible to select closely spaced fixed frequencies for the Fourier transform and the subsequent data analysis. In this work, 0.02Hz

frequency spacing is adjustable, which gives 50 frequencies evenly distributed on the interval 0.02-1.0Hz in each transformed time domain signal.

For longitudinal and lateral-directional combining aircraft dynamics, the state vector x, input vector u, and output vector y in (1) and (2) are defined by

$$x=\left[\alpha\ u\ q\ \theta\ \beta\ p\ r\ \phi\right]^T, \tag{15}$$

$$u=\delta_e. \tag{16}$$

System matrices containing the model parameters are:

$$A=\begin{bmatrix} A_1 & \vdots & 0 \\ \cdots & & \cdots \\ 0 & \vdots & A_2 \end{bmatrix}, \tag{17}$$

$$B=\begin{bmatrix} X_{\delta_e} \\ \dfrac{Z_{\delta_e}}{u_0} \\ M_{\delta_e}+\dfrac{M_{\dot\alpha}}{u_0}Z_{\delta_e} \\ 0 \\ 0 \\ L_{\delta_e} \\ N_{\delta_e} \\ 0 \end{bmatrix}, \tag{18}$$

$$A_1=\begin{bmatrix} X_u & X_\alpha & 0 & -g\cos\theta_0 \\ \dfrac{Z_u}{u_0} & \dfrac{Z_\alpha}{u_0} & 1 & 0 \\ M_u+\dfrac{M_{\dot\alpha}}{u_0}Z_u & M_\alpha+\dfrac{M_{\dot\alpha}}{u_0}Z_\alpha & M_q+M_{\dot\alpha} & 0 \\ 0 & 0 & 1 & 0 \end{bmatrix}, \tag{19}$$

$$A_2=\begin{bmatrix} Y_v & Y_p & Y_r & g\cos\theta_0 \\ L_v^*+\dfrac{I_{xz}}{I_{xx}}N_v^* & L_p^*+\dfrac{I_{xz}}{I_{xx}}N_p^* & L_r^*+\dfrac{I_{xz}}{I_{xx}}N_r^* & 0 \\ N_v^*+\dfrac{I_{xz}}{I_{zz}}L_v^* & N_p^*+\dfrac{I_{xz}}{I_{zz}}L_p^* & N_r^*+\dfrac{I_{xz}}{I_{zz}}L_r^* & 0 \\ 0 & 1 & 0 & 0 \end{bmatrix}. \tag{20}$$

5. RESULTS OF PARAMETER ESTIMATION AND FAULT ISOLATION

Figs. 9-12 show the comparison between the flight test data and the linear simulation results of FTR under the normal mode and the fault mode. Fig. 9 shows one of normal mode, Figs. 10-12 reveal the fault modes. Figs. 13-16 display the scatter diagrams of the estimated aerodynamic coefficients for several flight cases.

Table 3 shows the stability and control derivatives estimated from the flight test data for the normal and the fault mode by using the FTR method and the

Table 3. The comparisons of estimated stability/control derivatives for longitudinal motion.

	Normal Mode			Normal Mode (Mean)	Fault Mode				
	DATCOM Method	AAA Method [16]	FITLAB Method		-15deg	-7.5deg	0deg	+7.5deg	+15deg
TAS					121.2ft/s	117.6ft/s	116.9ft/s	126.6ft/s	117.9ft/s
H					233.1ft	418.1ft	621.0ft	266.3ft	207.3ft
C_{D_0}	0.0292	0.0377	0.1196	0.0988	0.1571	0.0475	0.1849	0.1929	0.1640
C_{D_α}		0.1725	0.1688	0.5254	1.3515	0.6604	1.4896	0.1140	-0.1453
C_{L_0}	0.4139	0.6245	0.3562	0.4494	0.3725	0.3651	0.2957	0.3012	0.4406
C_{L_α}	5.2431	5.5138	4.1544	5.0869	2.8664	3.7200	0.9285	2.1335	3.1999
$C_{m_{\dot\alpha}}$	-3.1311	-4.0938	35.1935	-23.8608	-8.1892	-18.0386	-15.3072	-3.8473	-9.3210
C_{m_α}	-1.8677	-1.6219	-0.5873	-0.6997	-0.4688	-0.5179	-0.4694	-0.3801	-0.4333
C_{m_q}		-22.5287	-63.6936	-30.2004	-23.6057	-24.2736	-29.6648	-19.3658	-17.4347
$C_{D_{\delta e}}$		0.0105	0.0058	-0.1632	-0.2159	-0.2212	-0.5820	0.1442	-0.0894
$C_{L_{\delta e}}$		0.2649	-0.0630	-0.2540	-0.2331	-0.1459	-0.4503	-0.3840	-0.1623
$C_{m_{\delta e}}$		-1.1879	0.8003	-0.3822	-0.2193	-0.1709	-0.2089	-0.1855	-0.1458
$C_{l_{\delta e}}$				0.0015	0.0064	0.0022	0.0024	0.0040	-0.0004

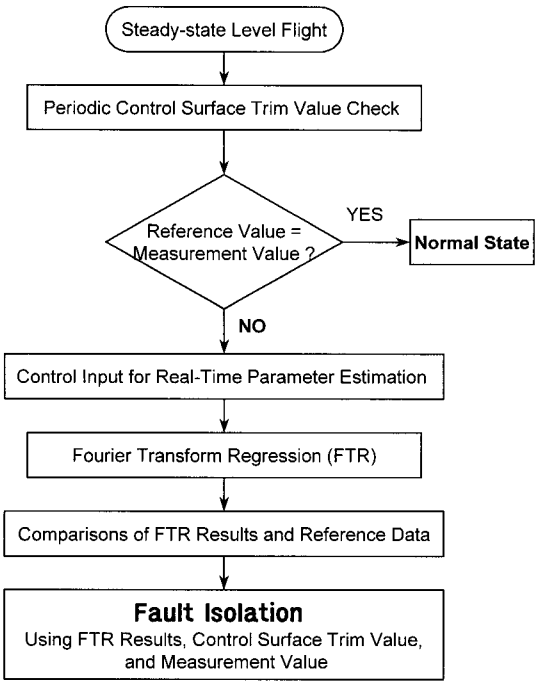

Fig. 8. Fault detection and isolation procedure include autopilot system.

Table 4. Straight level flight trim value of normal and fault mode.

Flight Condition	Elevator	Aileron	Rudder
Normal mode	0.9861deg	-0.3999deg	0.1736deg
Fault mode I	1.4815deg	-0.4068deg	0.0432deg
Fault mode II	-4.5282deg	-0.3853deg	0.3907deg
Fault mode III	-8.4626deg	-0.3226deg	0.8320deg
Fault mode IV	4.4312deg	-0.3595deg	0.2875deg
Fault mode V	7.4793deg	-0.3445deg	0.3311deg

FITLAB, which implements maximum likelihood parameter estimation of the general nonlinear system. Matlab toolbox FITLAB requires Matlab 5.3, Simulink 3.0, and Control System Toolbox 4.2. The aerodynamic coefficients computed from the analytical methods of the Advanced Aircraft Analysis [19] (AAA) and DATCOM are also included in these tables for the comparison.

The coefficient slop C_{L_α} estimated by the FTR is similar to the AAA and DATCOM. The segregated pattern of C_{L_α} in Fig. 13 tells that the normal and fault states can be identified from the normal mode and the fault mode. The change in pitching moment coefficient with respect to $\dot{\alpha}$, $C_{m_{\dot{\alpha}}}$ estimated by the FTR disagrees with the result of the AAA and DATCOM. Also, the $C_{m_{\dot{\alpha}}}$ in Fig. 14 shows that the normal and fault state slightly differs from the normal mode and the fault mode. The longitudinal static

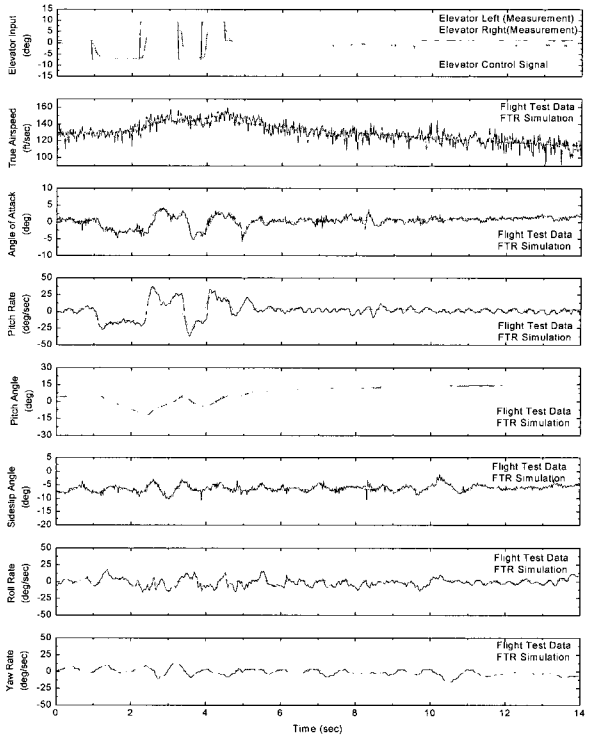

Fig. 9. Time histories from estimated stability/ control derivatives (normal mode).

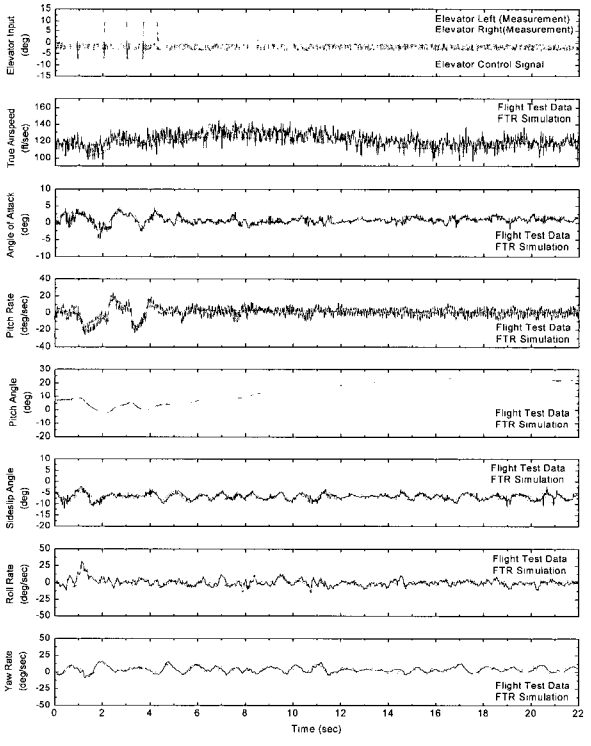

Fig. 10. Time histories from estimated stability/ control derivatives (fault mode I: 0deg).

stability parameter C_{m_α} is smaller than the AAA and DATCOM in the normal mode. The C_{m_α} in Fig. 15 indicates that the normal and fault state slightly differs

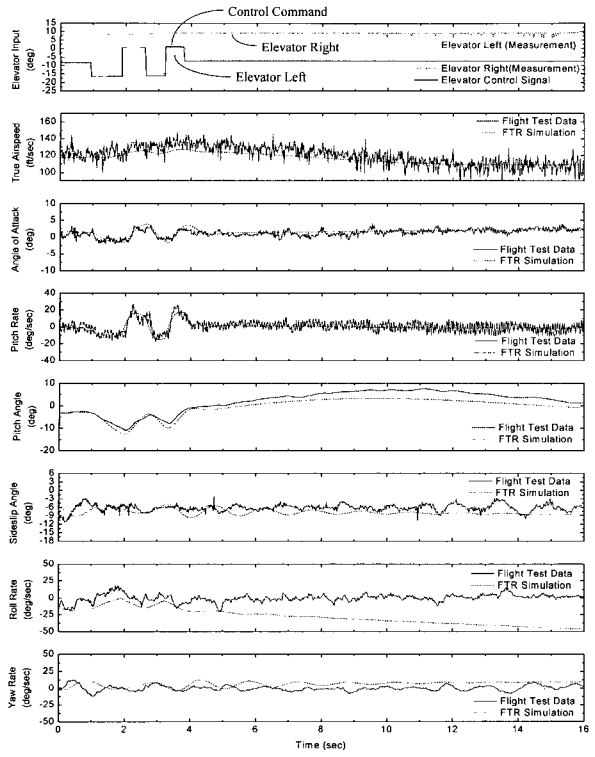

Fig. 11. Time histories from estimated stability/ control derivatives (fault mode III: -15deg).

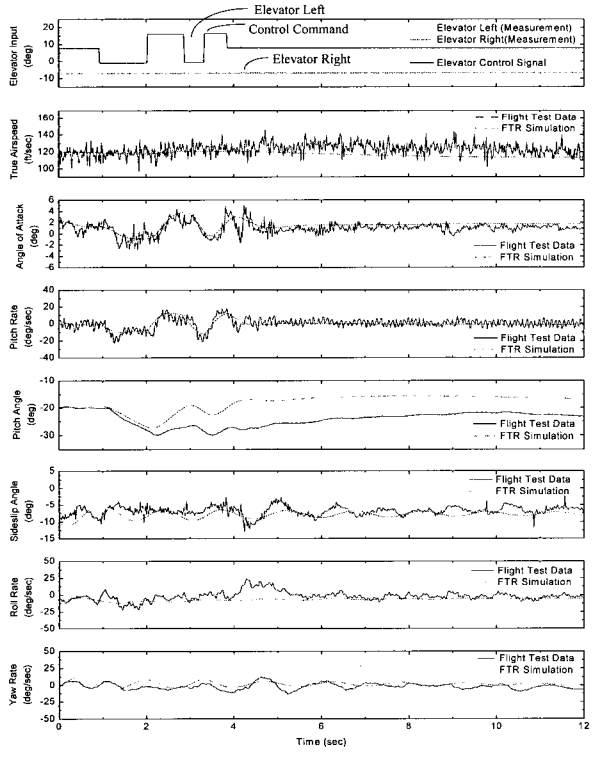

Fig. 12. Time histories from estimated stability/ control derivatives (fault mode V: +15deg).

from the normal mode and the fault mode. The $C_{m_{\delta_e}}$ estimated by the FTR is larger than the AAA in the

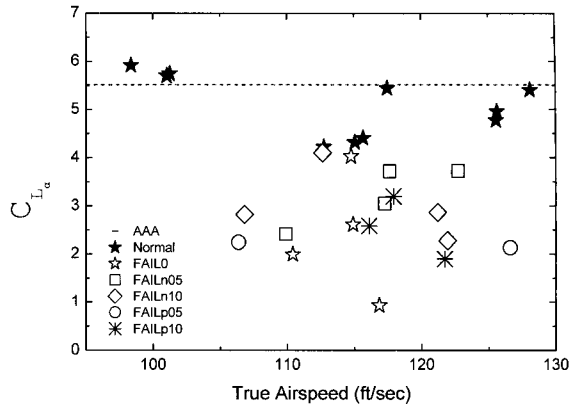

Fig. 13. Scatter of C_{L_α}.

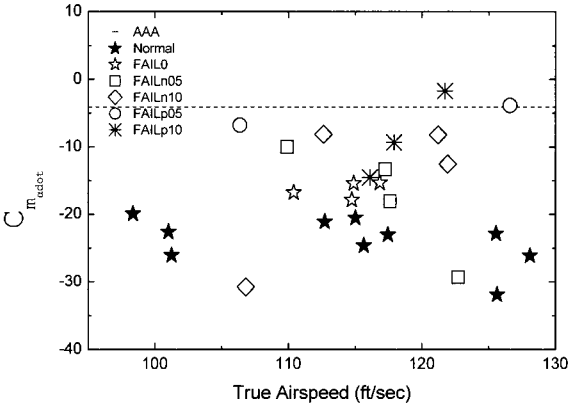

Fig. 14. Scatter of $C_{m_{\dot{\alpha}}}$.

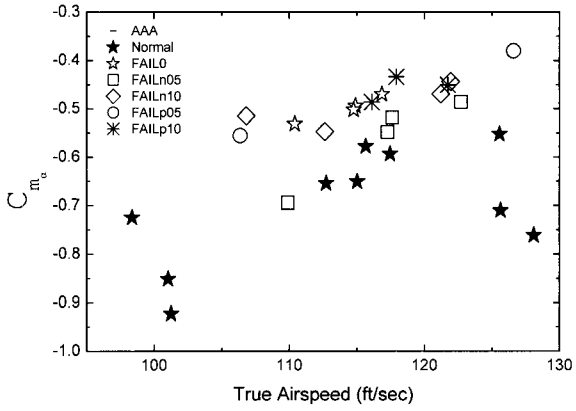

Fig. 15. Scatter of C_{m_α}.

normal mode. It clearly classifies the difference between the normal mode and the fault mode. Without the relation between the right elevator fault angle of -15deg, -7.5deg, 0deg, +7.5deg, and +15deg, the malfunction of the elevator reduces the elevator effect to half. The $C_{m_{\delta_e}}$ reduces the malfunction of the elevator by half, as shown in Fig. 16. Though Figs. 13-15 reveal that the normal and fault states differ, it is not satisfactory to determine the normal and fault

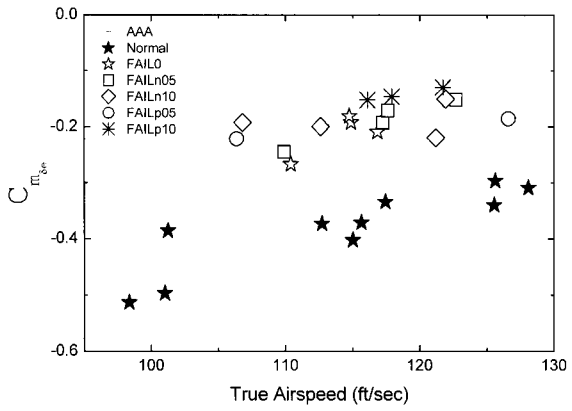

Fig. 16. Scatter of $C_{m_{\delta e}}$.

state with a pattern of C_{L_α}, $C_{m_{\dot{\alpha}}}$, and C_{m_α}, because it is difficult to estimate the variation of coefficients for the normal and fault states.

The straight level flight trim value of the DURUMI-II is presented in Table 4. The fault detection and isolation procedure is shown in Fig. 8. In Mode I to Mode V, the Fight Control Computer (FCC) recognizes that the elevator trim is changed and the $C_{m_{\delta e}}$ is only reduced by half. It is shown to be possible to detect the elevator fault by monitoring the elevator trim value and the control derivative value.

6. CONCLUSIONS

Using the remote control transmitter programming and switching method is a good way of reducing the cost, the time, and the effort for flight testing. The aerodynamic derivatives for the DURUMI-II were estimated from the flight test data by using the FTR for the normal mode and the fault mode with the fixed right elevator, and were compared with the results from the analytical prediction method. On the whole, The FTR results of the C_{L_α} from the flight test data in normal mode agree well with the analytical results from AAA, excluding the $C_{m_{\dot{\alpha}}}$ and C_{m_α}.

It is shown to be possible to detect the elevator fault by monitoring the value of the elevator trim and the value of control derivative $C_{m_{\delta e}}$ estimated in real time by the computer onboard the UAV during the flight.

For further study, additional flight tests will be performed to investigate the parameter variations for various failure conditions, and the fault case of lateral control surfaces such as rudder and aileron will also be tested and analyzed.

REFERENCES

[1] L. Ljung, *System Identification: Theory for the User*, Prentice Hall, Englewood Cliffs, NJ, 1987.

[2] W.-J. Park, *Parameter Estimation of Aerodynamic Stability Derivatives using Extended Kalman Filter (Longitudinal Motion)*, Master of Science, Hankuk Aviation University, December 1997.

[3] M.-S. Hwang, H.-B. Eun, W.-J. Park, Y.-C. Kim, K.-J. Seong, E.-T. Kim, and J.-W. Lee "Lateral stability/control derivatives estimation of canard type airplane from flight test," *Proc. of International Conference on Control, Automation and Systems*, 2001.

[4] M.-S. Hwang, W.-J. Park, Y.-C. Kim, H.-B. Eun, W.-J. Choi, and Y.-K. Song "Lateral stability improvement of a canard airplane using a vertical panel," *Proc. of AIAA Atmospheric Flight Mechanics Conference and Exhibit*, AIAA-2002-4625, Monterey, California, August 2002.

[5] W.-J. Park, *A Study on the Design of Real-Time Parameter Estimator for an Aircraft*, Ph.D. Thesis, Hankuk Aviation University, December 2004.

[6] A. Gelb, *Applied Optimal Estimation*, The M.I.T. Press, 1974.

[7] J. M. Mendel, *Lessons in Digital Estimation Theory*, Prentice-Hall, 1987.

[8] J. B. Garcia-Velo, *Parameter Estimation of an Unstable Aircraft Using an Extended Kalman Filter*, M.S. Thesis, University of Cincinnati, 1991.

[9] J. B. Garcia-Velo and B. K. Walker, "Aerodynamic parameter estimation for high performance aircraft using extended kalman filter," *J. Guidance, Control and Dynamics*, vol. 20, no. 6, pp. 1257-1260, Sept.-Oct. 1997.

[10] E. A. Morelli, "High accuracy evaluation of the finite fourier transform using sampled data," NASA-TM-110340, National Aeronautics and Space Administration, 1997.

[11] E. A. Morelli, "In-flight system identification," *Proc. of the AIAA Atmospheric Flight Mechanics Conference*, AIAA-98-4261, Boston, MA, August 1998.

[12] E. A. Morelli, "Real-time parameter estimation in the frequency domain," *Proc. of the AIAA Atmospheric Flight Mechanics Conference*, AIAA-99-4043, Portland, OR, August 1999.

[13] E. A. Morelli, "Identification of low order equivalent system models from flight test data," NASA-TM-210117, National Aeronautics and Space Administration, 2000.

[14] Y. Song, "A study on real-time aircraft parameter estimation," *Proc. of the KSAS Spring Annual Meeting*, pp. 359-362, 2001.

[15] M. R. Napolitano, Y. Song, and B. Seanor, "On-line parameter estimation for restructurable flight control systems," *Aircraft Design*, vol. 4,

no. 1, pp. 19-50, March 2001.
[16] S.-O. Koo, C.-H Im, K.-W. Nam, and H.-C. Lee "A study on comparison of dynamic stability and flight test for small-long endurance UAV," KARI-UA-TM-2000-010, Korea Aerospace Research Institute, June 2000.
[17] Y.-D. Kim, "A study on fault detection and redundancy management system," SUDP-P1-G4, Ministry of Commerce, Industry and Energy of Korea, March 2005.
[18] D. P. Raymer, *Aircraft Design: A Conceptual Approach*, AIAA Education Series, 1989.
[19] *Advanced Aircraft Analysis User's Manual Version 2.2*, DARcorporation, 1999.
[20] *Introduction to Performance and Flying Qualities Flight Testing*, National Test Pilot School, 2000.
[21] W.-J. Park, E.-T. Kim, K.-J. Seong, and Y.-C. Kim, "A study on the parameter estimation of DURUMI-II for the fixed right elevator using flight test data," *Journal of Mechanical Science and Technology*, vol. 20, no. 8, pp. 1234-1241, 2006.

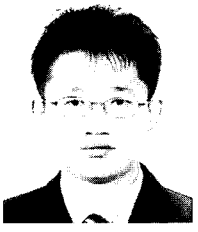

Wook-Je Park received the B.S. and Ph.D. degrees, both in Aeronautical Engineering, from Korea Aerospace University in 1994 and 2005, respectively. He is now a BK Research Professor at the School of Mechatronics, Changwon National University. His research interests are in fault detection and isolation, real-time parameter estimation method, flight testing, and their application in aircraft and UAV.

Eung-Tai Kim received the B.S. degree in Aeronautical Engineering from Seoul National University in 1981, the M.S. degree in Aeronautical Engineering from KAIST in 1983 and the Ph.D. degree in Aeronautical Engineering from Purdue University, West Lafayette in 1991. He is now a Principal Research Engineer at KARI. His research interests are in controller design, modeling and simulation, parameter estimation, flight testing, and their application in aircraft.

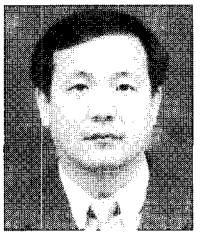

Yong-Kyu Song received the B.S. and M.S. degrees in Aeronautical Engineering from Seoul National University in 1985, and the Ph.D. degree in Aerospace Engineering from the University of Michigan, in 1992. He is now a Professor at the School of Aeronautical & Mechanical Engineering, Korea Aerospace University. His research interests are in control of aerospace vehicles, missile autopilot design, space trajectory analysis, control and analysis of nonlinear systems, and flight test data analysis.

Bong-Jin Ko received the B.S. degree in Telecommunication Engineering from Korea Aerospace University in 1986 and the M.S. and Ph.D. degrees in Electronic Engineering from Korea Aerospace University in 1988 and 1995, respectively. From 1994 to 1996, he was an Assistant Professor at Inha Technical College. He is currently a Professor in the School of Mechatronics, Changwon National University. His research interests are HAPS and satellite communication systems.